Vesicular stomatitis virus is a potent agent for the treatment of malignant ascites

YI ZHOU, FENG WEN, PENGFEI ZHANG, RUILEI TANG and QIU LI

Department of Medical Oncology, Cancer Center, State Key Laboratory of Biotherapy, West China Hospital, Sichuan University, Chengdu, Sichuan 610041, P.R. China

Received September 1, 2015; Accepted September 26, 2015

DOI: 10.3892/or.2015.4522

Abstract. Cancer cells in ascites are usually exposed to a hypoxia tumor microenvironment and utilize enhanced glycolysis which produces energy and metabolizes nutrients to support proliferation. Vesicular stomatitis virus (VSV) is an oncolytic virus that relies on the host cellular metabolism for replication. We tested the efficacy of VSV on peritoneal carcinomatosis and assessed VSV replication in cancer cells from ascites. BALB/c female mice bearing peritoneal H22 or MethA cells received an i.p. administration of $1x10^8$ PFU VSV or $1x10^8$ PFU equivalent of UV-inactivated VSV on day 10, 12 and 14 after incubation. Administration of VSV resulted in a significant inhibition of ascites formation and prolonged survival of the treated mice. The replication of VSV was obviously enhanced in the cancer cells from the ascites. Considering the central carbon metabolic pathways, cancer cells in the malignant ascites provided more exogenous glucose, glutamine and pyruvate after VSV infection due to its unregulated glycolytic activity and glutamine metabolism. Pharmacologically, inhibition of the glycolytic pathway and glutamine metabolism reduced VSV replication, and this inhibited replication was rescued by the addition of multiple tricarboxylic acid (TCA) cycle intermediates. Our results demonstrated that metabolic adaptive processes in peritoneal carcinoma, such as high glycolytic activity and glutamine metabolism, favor VSV replication. These results suggest the clinical potency of VSV in the treatment of malignant ascites and provide new insights into the further exploration of the potential application of VSV in the treatment of hypoxia ascites cancer cells.

Correspondence to: Dr Qiu Li, Department of Medical Oncology, Cancer Center, State Key Laboratory of Biotherapy, West China Hospital, Sichuan University, 37 GuoXue Xiang, Chengdu, Sichuan 610041, P.R. China
E-mail: qiuli108@yahoo.com.cn

Abbreviations: NS, 0.9% NaCl solution; i.p., intraperitoneally; TUNEL, fluorescent *in situ* terminal deoxynucleotidyl transferase dUTP nick end labeling; VSV, Δ51M recombinant IFN-inducing mutant of wild-type vesicular stomatatis virus (Indiana strain); PFU, plaque-forming units; RBC, red blood cell

Key words: vesicular stomatitis indiana virus, ascites, apoptosis, glycolysis, virus replication

Introduction

Cancer cells in ascites fluid are known to grow under highly anaerobic conditions. Previous research has shown that pO_2 in animal or patient malignant ascites is very low (1-3). Established tumor cells in ascites grow under highly crowded, virtually anoxic conditions (4-6). Under a hypoxic condition, cancer cells develop an efficient adaptive metabolic response to ensure their survival and proliferation. Glutamine and glucose represent the two main carbon sources for mammalian cells. In hypoxic cancer cells, glucose uptake and glycolytic activity are upregulated to produce pyruvate, which is then converted into lactate instead of being oxidized via the tricarboxylic acid cycle and oxidative phosphorylation (OXP HOS) (7). More recently, it has been shown that hypoxic cancer cells also exhibit an elevated glutamine demand and utilization to support cell proliferation through a glucose-independent tricarboxylic acid (TCA) cycle pathway (8-10). Cancer cells in malignant ascites favor a switch to glucose and glutamine-dependent anaerobic metabolic pathways, allowing adaptation to this microenvironment and promoting growth.

Viruses are dependent on the metabolic machinery of the host cell to supply the energy and molecular building blocks needed for genome replication, viral protein synthesis and membrane production. Extensive reprogramming of central carbon metabolism to induce the glycolytic pathway or glutamine metabolism has been observed during viral infection to meet virus replication requirements (11-15). Moreover, various studies have shown that hypoxia affects the replication of certain viruses (16-19). These studies demonstrate that the specific host cellular metabolism may be essential for maximal viral replication.

Vesicular stomatitis virus (VSV) is an oncolytic virus that replicates rapidly in tumor cell lines. A previous study showed that VSV can effectively replicate in hypoxic tumor cells *in vitro* and *in vivo* (20). Based on these findings, we asessed the oncolytic effect of VSV on carcinoma cells in malignant ascites and explored the impact of cellular metabolism on VSV replication.

Materials and methods

Vesicular stomatitis virus and cell lines. Two tumor cell lines were used in the experiments: hepatocellular carcinoma cell line H22 and retroperitoneal sarcoma cell line MethA. Both cell lines were obtained from the American Type Culture Collection (ATCC; Rockville, MD, USA). They were maintained in RPMI-1640 medium or Dulbecco's modified Eagle's medium (DMEM) tissue culture medium. Media were supplemented using 10% fetal bovine serum (FBS) (Gemini), 1% glutamine and 1% antibiotic mixture (Cellgro) unless indicated otherwise. Cells were grown in a humidified atmosphere containing 5% CO_2 at 37˚C. These two cell lines have the capacity to grow intraperitoneally (i.p.) in BALB/c female mice.

Δ51M recombinant IFN-inducing mutants of wild-type VSV were used in the animal study and they showed no toxic and durable cures in a previous study (21). VSV-Δ51 expressing GFP was a recombinant derivative of VSV-Δ51, and kindly provided by Yan-Jun Wen (Sichuan University). Plaque-forming units (PFU) were used for calculating infectious titers. Inactivated virus was produced by exposure to UV light for 45 min. Viruses were propagated in A549 cells (ATCC) and purified as previously described (22).

For viral infection, 24 h after seeding, the medium containing FBS was removed and replaced by serum-free medium 24 h before infection at a multiplicity of infection (MOI) of 1.0. One hour later, the infection medium was removed and replaced by complete serum-free medium with or without 600 mg/l L-glutamine, 2.5% glucose or 110 mg/l sodium pyruvate as indicated. Culture media were supernatants and cells were harvested at 0, 12, 24 and 48 h post-infection and processed for metabolites and protein quantifications. At each time point the cellular proteins were extracted, and cell supernatants were analyzed.

Plaque assay for VSV. The virus was purified from the supernatants by passing through a 0.2-μm filter and centrifuging at 30,000 x g, and then re-suspension in PBS. After A549 tumor cells were challenged with VSV at infection of 1.0 PFU/cell for 24 h, the supernatant was harvested for a progeny virus assay. PFU were used for calculating infectious titers as previously described (23).

Antibodies and inhibitors. β-actin antibodies were purchased from Sigma (Milano, Italy). VSV whole-virus antisera was provided by Yan-Jun Wen (Sichuan University). Sodium oxamate, 2-deoxy-D-glucose (2-DG), pyruvate, bis-2-(5-phenylacetamido-1,3,4-thiadiazol-2-yl)ethyl sulfide (BPTES) and dimethyl-α-ketoglutarate were purchased from Sigma. 2-DG and oxamate were directly solubilized in cell culture medium and BPTES was solubilized in dimethyl sulfoxide (DMSO) to a stock concentration of 10 mM, used at specified concentrations. In this research, all of the antibodies were used at the manufacturer's recommended dilution.

In vitro experiments. After 3 weeks of incubation, ascites cells were collected, washed with phosphate-buffered saline (PBS) three times, and used fresh for assays as described previous (24,25). After washing, the H22 and MethA cells from the ascites were used for further study immediately or maintained in RPMI-1640 medium. They were grown in a sealed modular chamber flushed with contained 5% CO_2 at 37˚C. For *in vitro* experiments, cells obtained from ascites were counted to $1x10^5$ cells per milliliter medium and cultured in 6-well plates, 24-well plates or 10-cm dishes. When the H22 and MethA cells were incubated for 12 h, they were treated with VSV as previously described (26). In brief, the virus was added to the culture at an MOI of 1.0 PFU per cell. After VSV incubation for 1 h at 37˚C, the cells were washed once with PBS and 5 ml of RPMI-1640 or DMEM. Following incubation, the cells were maintained for an additional period of 0-48 h and harvested, washed 3 times with PBS, scraped into RIPA buffer, centrifuged at 8,000 rpm at 4˚C for 10 min and stored at -80˚C for further analysis, and the media were collected to conduct further investigation. At the end of the incubation period, viable cells in each well were counted using the trypan blue method and the final results were normalized as described.

mRNA determinations. Total RNA was isolated by an Isogen RNA extraction kit (Nippon Gene, Inc., Tokyo, Japan) and reverse-transcribed by murine leukemia virus reverse transcriptase using a High Pure RNA Isolation kit (Invitrogen, Sydney, Australia) according to the manufacturer's protocol. cDNA amplicons were amplified with specific primers (data not shown). We used the β-actin gene as an internal control (202 bp; β-actin sense, 5V-CTTCCTGGGCATGGAGTCCT-3V; antisense, 5V-GGAGCAATGATCTTGATCTT-3V). The amplification was carried out in a Palm Cycler. The initial cDNA synthesis was performed at 54˚C for 30 and 5 min at 94˚C for denaturation. This was followed by 30 rounds of amplification of PCR consisting of 1 min at 94˚C, 1 min at 55˚C, 2 min at 72˚C with a Gene Amp PCR System 9600 (Perkin Elmer) and *Taq* DNA polymerase (Toyobo, Osaka, Japan). The amplified DNA fragments were visualized by electrophoresis at 120 V on 2% agarose-gel in 1X TAE buffer containing ethidium bromide. DNA molecular weight marker was also electrophoresed for comparison.

Glucose, glutamine and pyruvate quantifications. Metabolites were quantified from cell supernatants using a Glucose (GO) Assay kit, a Glutamine Determination kit (GLN1) (Sigma-Aldrich, Saint-Quentin Fallavier, France) and a pyruvate assay kit (BioVision, Nanterre, France). Assays were performed according to the manufacturer's instructions. At each time point the cellular proteins were extracted, and cell supernatants were analyzed. For each assay, concentrations in the cell culture medium were normalized with total protein amounts in the well and are expressed as nmol consumed (compared to time zero) per μg of protein (nmol/μg).

Western blot analysis. For western blot analysis, protein samples were subjected to 10% sodium dodecylsulfate-polyacrylamide gel electrophoresis (PAGE) and transferred to a nitrocellulose membrane. The membrane was blocked with 5% skim milk in TBS [20 mM Tris and 137 mM NaCl (pH 7.3)] containing 0.1% Tween-20, and then the membrane was incubated with the specific antibodies. After being washed, the membrane was incubated with

peroxidase-conjugated goat anti-mouse immunoglobulin G or anti-rabbit immunoglobulin G. Kodak Molecular Imaging software was used to quantification the intensity of the bands (Eastman Kodak Co., Rochester, NY, USA).

Quantitative assay of VEGF in ascites fluid and plasma. After obtaining the cell-free supernatants of ascites and plasma of mice, VEGF levels were measured with ELISA kits (Quantikine; R&D Systems, Minneapolis, MN, USA) as described by the manufacturer's protocol.

Flow cytometry. Malignant ascites H22 and MethA or cells obtained from ascites or cultured in a dish were infected with GFP-VSV as previously described. To evaluate infectivity, GFP fluorescence intensity was measured by flow cytometry 48 h after incubation; data were analyzed using FLOWJO software. For analysis of apoptosis, flow cytometric analysis (FCM) was performed to detect sub-G1/apoptotic cells in hypotonic buffer as previously described (24).

TUNEL. Fluorescent *in situ* terminal deoxynucleotidyl transferase dUTP nick end labeling assay was used to analyze the apoptotic cells within malignant ascites or cultured cancer cells after VSV infection using a commercially available apoptotic cell detection kit (Promega, Madison, WI, USA). After the cells were incubated with the VSV for 48 h, the cells were rinsed with PBS 3 times. The samples were counted to $1x10^6$ cells and subsequently spread on a slide to perform TUNEL assay following the manufacturer's protocol.

Murine tumor models. BALB/c female mice were used to establish H22 and MethA cell models, respectively. Before injection, the mice were housed in autoclaved microisolator cages in specific pathogen-free conditions and fed autoclaved pellets and sterile water *ad libitum*. All animal research was approved by the Animal Care and Use Committee of Sichuan University and was in compliance with all regulatory guidelines. The health status of each animal was monitored daily. Following a week of acclimatization, the mice were injected i.p. with $10x10^6$ H22 and MethA cells. Malignant ascites was collected three weeks later, red blood cells were schizolysed, and ascites fluid free of red blood cells was washed with PBS three times and centrifuged at 300 x g at 4˚C for 5 min. Each type of tumor cell ($1x10^6$) suspended in 100 μl of PBS was then injected i.p. into the mice with a 14-gauge needle.

Treatment and sample collection. After approximately 7 days of cancer cell incubation, ascites formation was observed. On day 10, 12 and 14, the mice were treated with $1x10^8$ VSV-Δ51 or $1x10^8$ PFU equivalent of UV-inactivated VSV-Δ51 by intraperitoneal injection. Five mice from each group were left to develop ascites, and the weight of each mouse was recorded every other day until day 24 after implantion when the mice were euthanized. After euthanasia, the ascites fluid was collected, and the numbers of tumor cells and red blood cells were counted per milliliter per mouse. Before sacrifice, a blood sample was collected through the ophthalmic artery; ascites fluid was completely aspirated as previously described (24). The other five mice of each group were monitored on a daily basis for tumor burden, cachexia and abdominal distension. Mice were euthanized when their abdominal circumference reached 9.5 cm or they were becoming moribund. The survival time of each animal was calculated from the day of the beginning of the treatment to euthanasia. The ascites volume of each mouse was calculated as previously described (24). All of the specimens including cells, cell-free ascites fluid, tumors dissected from the peritoneal cavity and the plasma were stored in liquid nitrogen for further analysis. Ascites fluids of the control group were centrifuged and supernatants were liquidated into 1 ml samples and stored at -80˚C until needed.

Assessment of toxicity. The relevant indices concerning side effect, such as diarrhea, anorexia, skin ulceration, or cachexia were observed every day. The heart, liver, lung, spleen and kidney were harvested and fixed in 4% paraformaldehyde in PBS, then sectioned and stained with H&E. All of the sections were observed by two different pathologists.

Statistical analysis. All data are reported as the means ± SE. Comparison of the different group samples was carried out by analysis of variance (ANOVA) and an unpaired Student's t-test. The level of significance was set as $P<0.05$. We used standard statistical software SPSS, version 13, for all statistical analyses.

Results

In vivo inhibition of malignant ascite formation. To evaluate the effect of VSV on malignant ascite formation, mice bearing i.p. H22 and MethA tumor cells were treated with VSV 3 times on day 10, 12 and 14 after incubation. Using a well-established animal model of malignant ascites formation, here we showed an inhibitory effect of VSV on intraperitoneal tumor growth, malignant ascites formation. Fig. 1A shows the survival curves of the mice bearing H22 or MethA tumor cells from the three groups. In several mice, VSV treatment abolished the malignant ascites completely; nearly 80% survived the full intended length of study (40 days). In contrast, all of the mice from the NS and UV-VSV-treated group died by day 40, before the treatment period was over. At the end of the treatment period, the mean volume of ascites in the control groups was 7.44±1.45 and 4.76±0.63 ml per mouse in the H22 and MethA model, respectively. The mean volume of ascites in the VSV-treated groups were 1.09±0.45 and 1.06±0.66 ml per mouse ($P<0.05$); ascites in several mice were abolished completely (Fig. 1B). The health condition of the control mice was poorer than that of the treated group and exhibited anemia, asthenia or asitia. VSV treatment significantly reduced the number of floating tumor cells and the red blood cells ($P<0.05$) in the peritoneal cavity (Fig. 1C). In the H22 and MethA models only $41.6±4.21x10^6$ and $23.43±3.37x10^6$ tumor cells and $21.6±4.21x10^6$ and $35.43±3.37x10^6$ red blood cells per milliliter were found in the mice treated with VSV, while in the controls and UV-VSV group there were nearly 2-fold more tumor cells and 8-fold more red blood cells than that in the VSV-treated group. Therefore, treatment of VSV in the malignant models reduced the tumor burden and improved the health condition of the mice. Differences between the VSV and UV-VSV group achieved statistical significance

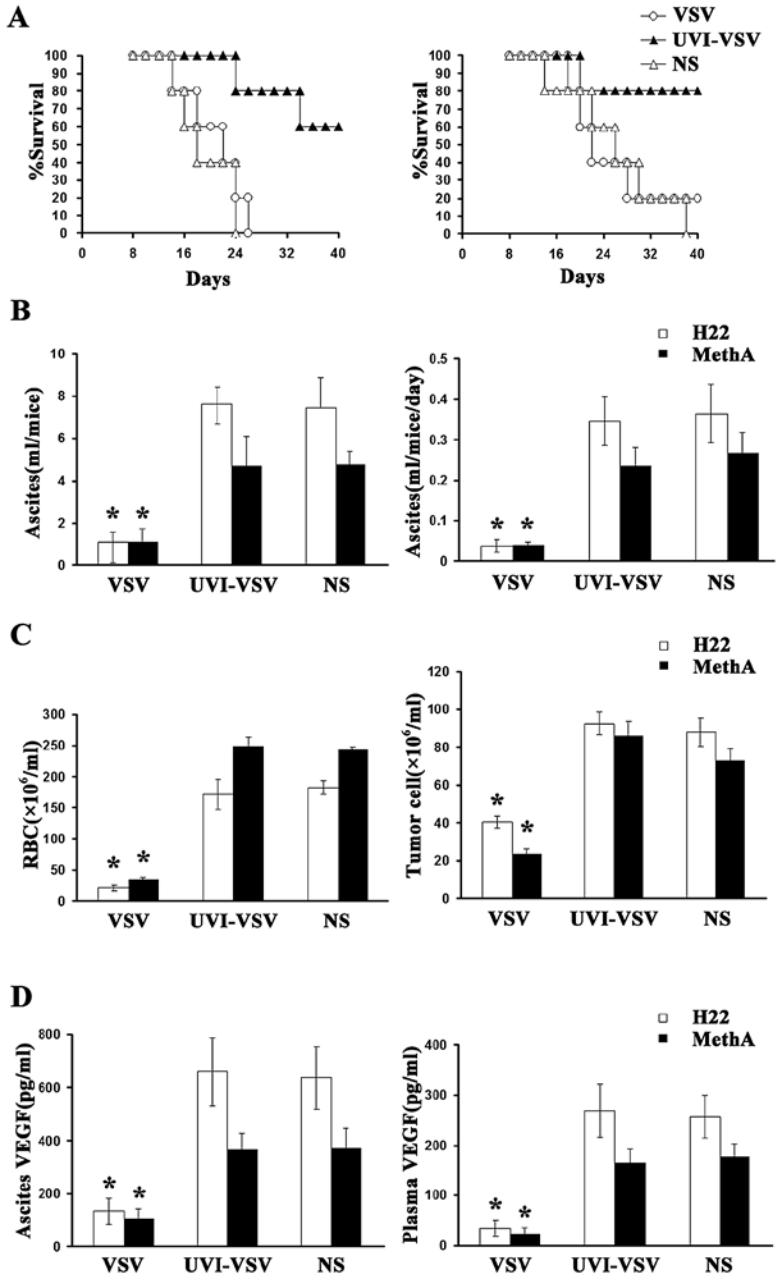

Figure 1. Treatment effect of VSV on malignant ascites in an H22 and MethA model. BALB/c female mice inoculated i.p. with H22 and MethA cells were randomly assigned to NS (100 μl of 0.9% normal saline), VSV-Δ51 or UV-inactivated VSV-Δ51 ($1x10^8$ PFU of VSV suspended in 100 μl of normal saline) treatment groups (n=10 per group). Mice were intraperitoneal injected on day 10, 12 and 14 after incubation. They were euthanized in the state of ill health or upon an abdominal circumference >9.5 cm. (A) Survival curves of the tumor-bearing mice are shown. The period in days lapsed between the beginning of treatment and euthanasia was calculated as survival, and the percentage of surviving mice was calculated as the number of animals remaining in each group. (B) The volume of ascites collected from the intraperitoneal was assessed to determine the total ascites volume for each mouse. (C) The tumor cell numbers present in the ascites of each group were counted when 5 mice of each group were euthanized on day 24 after incubation. (D) The VEGF levels in plasma and cell-free ascites of each group. ELISA kit was used to measure VEGF levels in plasma and cell-free ascites fluid in the VSV, UV-VSV or NS-treated mice (picograms of VEGF per milliliter was calculated); For all figures, P<0.05. Columns represent the mean values; error bars indicate SE.

(P<0.05). These results suggest that administration of VSV within the peritoneal cavity was sufficient to suppress malignant ascite formation and prolong survival time. This higher level of inhibition suggests that VSV is efficient for the treatment of ascites particularly in the late phase.

VSV decreases the VEGF level in plasma and ascites. VEGF is the most widely implicated growth factor involved in the initiation and progression of malignant ascite formation. We therefore measured VEGF (Fig. 1D) concentrations in plasma and ascites and found a significant decrease in the concentration levels in the treated mice. Compared to the values in the control group, plasma and ascite VEGF levels were significantly reduced. In the VSV-treated group total ascite VEGF levels decreased from 637.33±118.72 to 133.40±46.45 pg/ml (P<0.05) in the H22 group and 372.12±6.78l to 104.25±39.44 pg/ml (P<0.05) in the MethA group, respectively. Furthermore, the plasma VEGF level was significantly reduced from 257.72±43.26 in the control mice to 34.53±15.68 pg/ml (P<0.05) in the H22 group and from 175.45±26.76 in the control mice

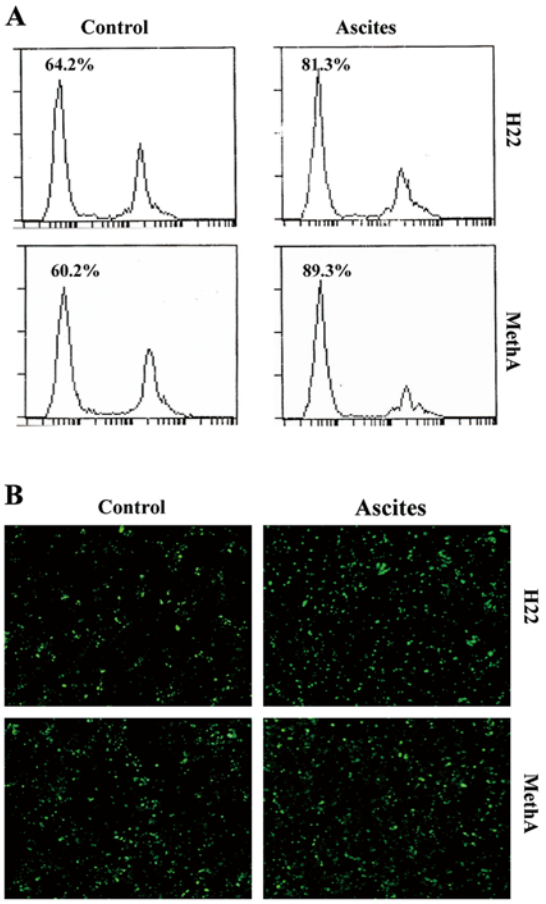

Figure 2. VSV induces the apoptosis of cancer cells from ascites. Malignant ascites from tumor-bearing mice of untreated group were collected, and then rinsed with PBS three times. After a 12-h incubation, cells were counted to $5x10^5$ cancer cells per milliliter of medium. Cultured cells and ascites cells were infected with VSV at an MOI of 1.0. (A) DNA fluorescence histograms of PI-stained ascites or cultured H22 and MethA cells were detected after 48 h of VSV infection. (B) The tumor cells were counted to $1x10^6$ cells per sample to be stained with FITC-dUTP as described in the text. Apoptotic nuclei (green) were identified by TUNEL and observed under a fluorescence microscope. Original magnification, x200.

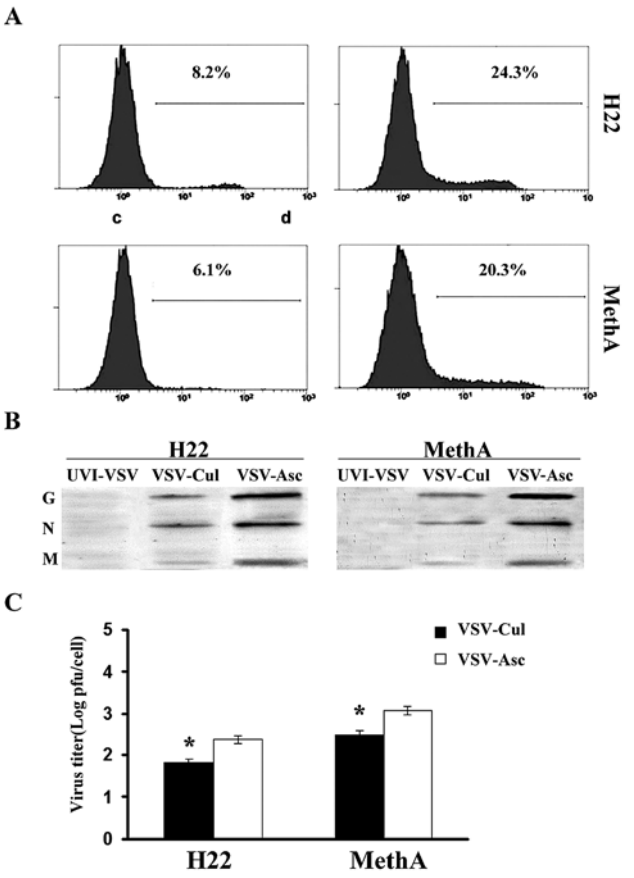

Figure 3. VSV replication was enhanced in H22 cancer cells from ascites. Ascites H22 cancer cells and dish-cultured H22 cancer cells were infected with VSV at an MOI of 1.0. (A) Cells were infected with VSV-Δ 51-GFP (1.0 MOI) for 1 h. Then, 24 h post-infection, the percentage of infected cells was determined by flow cytometric analysis of GFP expression as shown. (B) Immunoblot analysis of viral proteins (G, G protein of VSV; N, N protein of VSV; M, M protein of VSV) in ascites cancer cells and cultured cancer cells infected with VSV (MOI, 1.0; 24 h after infection). The blot was probed with a diluted rabbit anti-VSV serum. The expression of β-actin was used as an internal control. (C) The titers of infectious VSV in ascites cells and cultured cells were assayed in H22 or MethA cells at 24 or 48 h after infection. Assays were performed in triplicate wells. For all figures, $P<0.05$. Columns represent mean values; error bars indicate SD.

to 23.22±13.12 pg/ml ($P<0.05$) in the MethA group. Together, these results showed that VSV effectively blocks cancer and hypoxia-induced elevation of VEGF levels in these mice. This level of VEGF suppression is correlation with significant regression of disease within the peritoneal cavity.

VSV induces the apoptosis of H22 and MethA cells in malignant ascites. To investigate the apoptotic effect of VSV on the malignant ascites cells, we treated ascites cells and cultured cells with VSV. We used flow cytometry to assess the percentage of sub-G1 phase cells in order to estimate the number of apoptotic cells. Cells from the ascites exhibited increased apoptosis compared to the cells cultured in a dish treated with VSV (Fig. 2A). In malignant ascites of late phase, we showed that VSV induced cell apoptosis by 64.2% in the cultured H22 cells whereas in ascites H22 cells the rate of apoptosis was 81.3% after 48 h of infection. Regarding the MethA cells, the rate of apoptosis was 60.2% in the cultured cells whereas the rate was 89.3% in the ascites cells. Furthermore, TUNEL assay was also carried out to detect early DNA fragmentation associated with apoptosis (Fig. 2B). Although the apoptotic effects of VSV were variable among the different cells, cells from ascites illustrated increased apoptosis. Taken together, these results suggest that VSV induces a high rate of apoptosis in cells from malignant ascites fluid.

VSV replication is enhanced in the H22 and MethA cells from malignant ascites. To quantitatively analyze the expression of viral and cellular proteins, we performed viral infection at an MOI of 1.0 in the following experiments. We assessed the effect of VSV replication in the H22 and MethA cancer cells from the malignant ascites. H22 and MethA cells were infected with VSV-Δ 51-GFP as previously described. The expression of VSV-Δ 51-GFP in the H22 and MethA cells was examined using flow cytometry (Fig. 3A). We observed that VSV replication in malignant ascites H22 and MethA cancer cells was enhanced. Immunoblot analysis using anti-VSV serum also revealed higher levels of expression of VSV proteins in the cells from the ascites than that in cultured cells at 24 h after

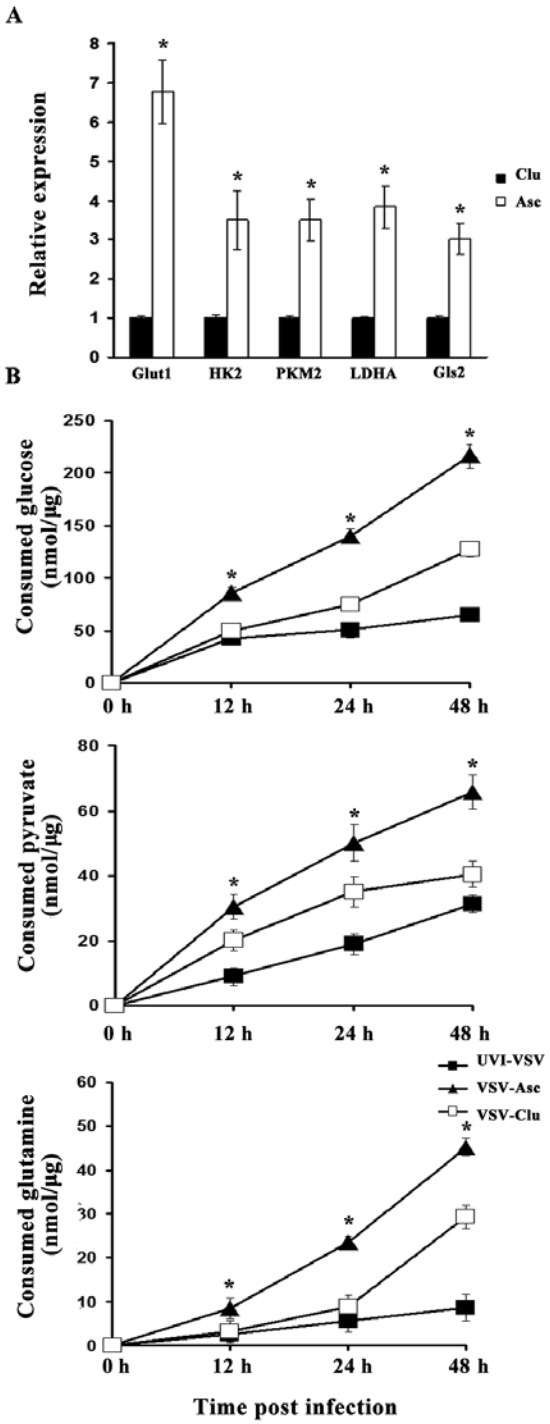

Figure 4. Consumption of metabolites after VSV infection in ascites and cultured H22 cells. (A) HK2, Glut1, PKM2, GLS2 and LDHA mRNA levels in ascites H22 cells and cultured H22 cells. The results were normalized to the values of the corresponding cultured cells in normoxia. (B) Ascites H22 cells and cultured H22 cells were serum starved for 12 h and subsequently mock infected or infected by VSV at an MOI of 1.0. Supernatants and cells were harvested at 0, 12, 24 and 48 h post-infection and processed for metabolite detection and protein quantifications. Consumption of glucose, glutamine and pyruvate by cells was calculated and normalized to total protein amounts in the well and are expressed as nmol consumed per μg of protein. For all figures, $P<0.05$. Columns represent mean values; error bars indicate SD.

VSV infection (Fig. 3B). Twenty-four hours following infection, the number of VSV-infected cells increased 2- to 4-fold in the H22 cells from the malignant ascites and 2- to 4-fold in the MethA cells from the malignant ascites (Fig. 3C) compared to the cultured cells. These results indicate that the production of viral proteins and the viral replication were enhanced in cancer cells from the malignant ascites.

H22 and MethA cells from the malignant ascites exhibit increased aerobic glycolysis and glutamine metabolism. Hypoxia promotes the shift from OXP HOS to a glycolytic mode, leading to increased glucose capture and lactic acid production by tumor cells (anaerobic 'glycolysis'). Here, we aimed to gain further insight into the glycolytic activity of malignant ascites H22 cells and compare this activity to that of normoxic cultured cells. We first investigated the expression of genes involved in glycolytic metabolism such as hexokinase 2 (Hk2), PKM2 and lactate dehydrogenasea (LDHA) as well as glucose transporters such as glucose transporter 1 (Glut1). We also determined the expression of glutaminase GLS2, the key enzyme which catalyzes glutamate production from glutamine in a hypoxic condition. All glycolytic activity was standardized to that noted in the nomoxia dish-cultured cells. The ascites H22 cells exhibited a relatively higher level of expression of all these genes than levels noted in the control cells cultured under normoxia, resulting in high glycolytic activity and glutamine metabolism. Statistical significance was found for GLUT1, PKM2, Hk2, GLS2 and LDHA ($P<0.05$). Of note, GLUT1 and LDHA are known to be responsible for increased glucose uptake and consumption via anaerobic glycolysis but not oxidative phosphorylation. The result indicates that cancer cells in malignant ascites are highly glycolytic and the glucose and glutamine consumption are elevated (Fig. 4A).

Glycolysis production and glutamine are consumed for efficient infectious VSV replication. It is known that viruses make use of cell nutrition for replication. We next assessed the three main carbon sources of hypoxia cells: glucose, glutamine and pyruvate. We then measured key metabolite consumption within the supernatants of the ascites or cultured H22 cells infected with VSV (MOI 1.0) or UVI-VSV at different times post-infection in the medium with indicated concentrations of glucose pyruvate lactate or glutamine (i.e., 0, 12, 24 and 48 h). Following infection with VSV, the consumption of glucose, glutamine and pyruvate was elevated because of virus replication (Fig. 4B). Interestingly, the consumption of glucose, pyruvate and glutamine in the VSV-infected ascites cancer cells was more rapid than that noted in the VSV-infected cultured cells. Moreover, the gap in consumption between the VSV infection and UVI-VSV infection in ascites cancer cells was much more obvious than that in the cultured cancer cells (data not shown).

Glycolysis is required for optimal infectious VSV production. Since pyruvate, glucose and glutamine are consumed for virus production, we hypothesized that glycolysis and glutamine metabolism are necessary for efficient viral replication. We investigated the impact of both glucose and glutamine deprivation on VSV replication. As expected, the replication of the virus was restrained in medium without glutamine or glucose, as shown in Fig. 5A, and replication of the virus was restored when glutamine or glucose was added. Thus, we next examined VSV replication following treatment with oxamate

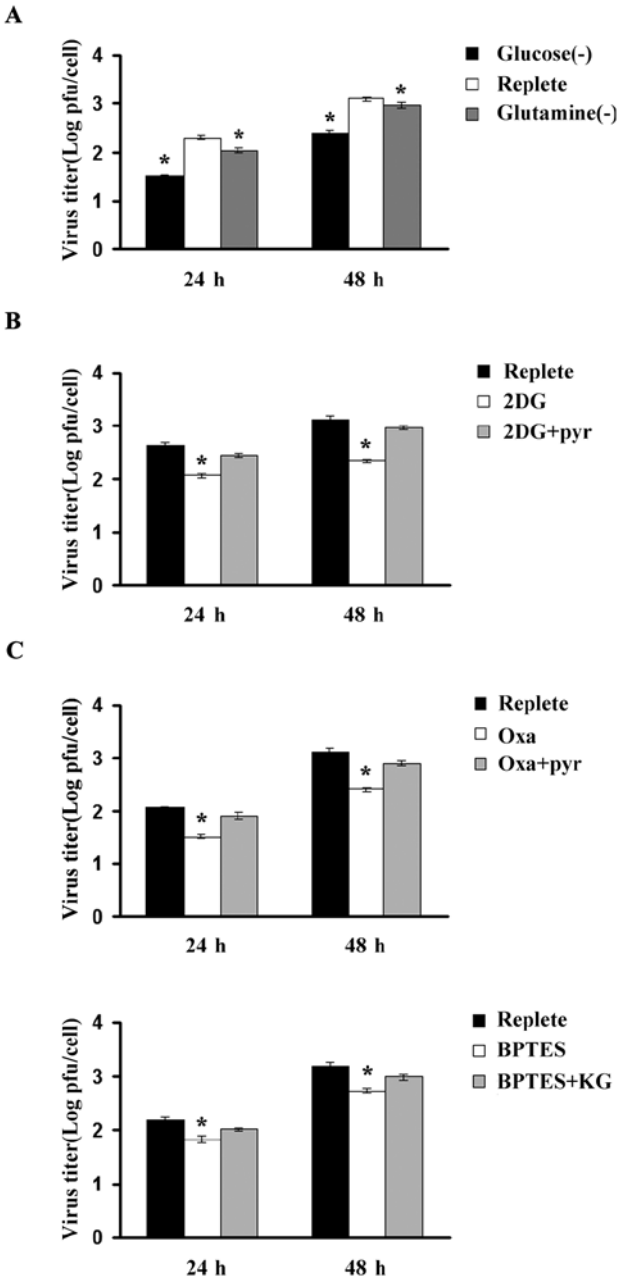

Figure 5. Glycolysis is required for maximal VSV replication. (A) Ascites H22 cells were infected with VSV at an MOI of 1.0 and were fed replete medium without glucose or glutamine (0 mM). Viral titers were quantified by plaque assay. The virus replication was restrained in glucose or glutamine-free medium. When glucose or glutamine was added to the medium the replication of viral was restored as shown. (B) Ascites H22 cells were infected with VSV at an MOI of 1.0 and were fed replete medium (0 mM) or replete medium supplemented with 2DG (2 mM) or oxamate 50 mM with or without or 4 mM pyruvate. Twenty-four hours post-infection, virus replication was quantified by focus-forming unit reduction assays. (C) Ascites H22 cells were infected with VSV at an MOI of 1.0 and were fed replete medium, or replete medium supplemented with 10 μM BPTES or with 10 μM BPTES and 7 mM dimethyl-α-ketoglutarate. Viral titers were detected as in B after 24 h of incubaton. For all figures, P<0.05. Columns represent mean values; error bars indicate SD.

and 2-DG, a glycolytic inhibitor. Oxamate is a pyruvate analog that can block the conversion of pyruvate to lactate or acetyl-CoA (27). 2-DG, a glucose analog that inhibits hexokinase, is the first enzyme in the glycolytic pathway. We first investigated the effect of 2-DG on glycolysis in the ascites H22 cancer cells. Glucose uptake, ATP production and pyruvate production were increased (data not shown) in the ascites cancer cells. VSV-infected ascites H22 cells treated with oxamate or 2DG exhibited a decrease in the release of extracellular infectious virus (Fig. 5B). Notably, the replication of the VSV was restored, when the medium was supplemented with 4 mM pyruvate. These data indicate that glycolysis is a critical metabolic pathway for optimal VSV replication.

Glutamine is involved in VSV replication in malignant ascites H22 cells. It has been shown that hypoxic cancer cells also use glutamine as a carbon fuel source for survival (28-30). Viruses require exogenous glutamine for efficient replication, and inhibition of glutamine metabolism blocks certain virus protein synthesis (14). We examined infectious virus replication following pharmacological inhibition of glutamine metabolism. VSV-infected cells were treated with BPTES to inhibit glutaminase, the key enzyme that catalyzes the first step of glutaminolysis, which converts glutamine to glutamate. Fig. 5C shows that blockage of glutaminolysis reduced viral replication. Moreover, virus production in the BPTES-treated cells was significantly recovered by α-ketoglutarate supplementation.

Discussion

We examined the effect of VSV on the suppression of malignant ascites accumulation, survival time and tumor burden in a H22 and MethA cell malignant ascites model. We found that VSV profoundly suppressed VEGF secretion and induced the apoptosis of ascites cancer cells. Furthermore, we found that the replication of VSV was enhanced in malignant ascites. We showed that cancer cells in malignant ascites increased the 'glycolytic' switch to produce pyruvate and elevate usage of glutamine as a carbon fuel source. The curative effect of VSV on malignant ascites may lie in the hypoxia-driven metabolic adaptive processes, such as high glycolysis rate, hexosamine biosynthetic pathway activation, and glutamine metabolism favoring vesicular stomatitis virus replication.

Virus replication depends on the metabolic machinery of the host cell to supply the energy and metabolize nutrients. In support of our metabolomic data, we showed that when the ascites H22 cells were infected by VSV, the consumption of glycolysis production and glutamine increased. In glucose-free media or after glutamine starvation, VSV replication was markedly increased in the ascites H22 cells. Interestingly, the blockage of glycolysis or glutamine metabolism was able to restain VSV replication, while addition of pyruvate or glutamine metabolite increased the VSV titer. Although the requirement of increased glycolysis production and glutamine metabolite for virus replication is clear, how glycolysis is utilized for viral replication remains to be determined. It is possible that enhanced glycolysis directly supports other replication needs, such as the generation of ATP and NADH.

More recently, it has been shown that hypoxic cancer cells also use glutamine as a carbon fuel source for survival. Previous research found that glutamine metabolism is considerably altered during viral infection and is necessary to anaplerotically replenish the TCA cycle (14,31), raising the possibility that glutamine also serves as an anaplerotic substrate for

the TCA cycle during VSV infection. However, glutamine is consumed in multiple metabolic pathways, providing the nitrogen for nucleotide biosynthesis. The observed blockage of virus production under conditions of glutamine deprivation could also be due to the fact that VSV requires glutamine as both a carbon source and a nitrogen source to support the replicative needs. Metabolic carbon and nitrogen flux analysis is warranted to gain further insight into global glucose and glutamine usage during VSV infection.

The data presented here demonstrated that inhibition of the glycolytic pathway via oxamate or 2-DG treatment resulted in a significant reduction in VSV replication. Our data coincided with other studies that found that the glycolytic pathway of glucose utilization is specifically altered during viral infection. Other laboratories have previously described that many human viruses activate glycolysis and dysregulate the expression and/or activity of GLUT1 and Hk2 after infection to facilitate glycolysis (12,32-36). Moreover, inhibition of the glycolytic pathway has been shown to restrict HCMV and HSV-1 replication and induce apoptosis in cells latently infected with KSHV (37-39). Viral replication may increase the demand of critical metabolite matters, which are provided by glycolytic pathway and glutaming metabolism to support their life cycles.

Under a hypoxic condition, a shifting of cellular metabolism to enhance the anaerobic state was observed. Activation of the PI3K/Akt pathway, Myc transcription factor and hypoxia-inducible factor 1 (HIF-1) under a hypoxic condition plays important metabolic roles in enhancing glycolysis or utilization of glutamine which upregulates genes involved in glucose uptake (GLUT1), anaerobic glycolysis (LDH-A, Hk2 and PKM2) and enhances the expression of glutaminase (GLS). It has been shown in previous studies that VSV selectively invades tumor cells with p53, Ras and Myc gene mutations (40,41). Those genes were transcriptional activate Hk2, pyruvate kinase under hypoxia in a HIF-independent manner. The requirement of glycolysis and glutamine metabolism in VSV replication made VSV metabolism targeted to hypoxia cancer cells. Furthermore, the oncolytic virus has been used in the treatment of peritoneally planted ascites tumor cells and an orthotropic model of bladder cancer (21,42,43), all of which were under a hypoxic environment. Intraperitoneal administration was well tolerated, and no severe adverse effects were observed, even using immunocompromised hosts. VSV instillation therapy in an orthotopic model of bladder cancer showed promising antitumor activity and safety (43).

VSV is expected to be applicable for cancer therapy as an oncolytic virus since the viral replication of VSV is enhanced in cancer cells compared with normal tissues. In the present study, replication of VSV was enhanced in ascites H22 and MethA cells. Enhancement of the viral replication in cancer cells from ascites is considered to be due to upregulation of glycolysis and glutamine metabolism in the hypoxic condition found in ascites. Thus, VSV metabolism is targeted to hypoxic cancer cells, implying that this oncolytic virus exhibits its anticancer ability efficiently under a hypoxic condition.

Acknowledgements

The present study was supported, in part, by the Project of the National Natural Science Foundation of China (no. 81071862).

References

1. Del Monte U: Considerations on factors influencing the oxygenation of ascites tumours. Eur J Cancer 5: 639-640, 1969.
2. Cheng B, Williams M and Chance B: Effects of glucose, anoxia, and adriamycin on the chemiluminescence of Ehrlich Ascites cells. FEBS Lett 160: 169-172, 1983.
3. Inoue M, Mukai M, Hamanaka Y, Tatsuta M, Hiraoka M and Kizaka-Kondoh S: Targeting hypoxic cancer cells with a protein prodrug is effective in experimental malignant ascites. Int J Oncol 25: 713-720, 2004.
4. Kuemmerle A, Decosterd LA, Buclin T, Liénard D, Stupp R, Chassot PG, Mosimann F and Lejeune F: A phase I pharmacokinetic study of hypoxic abdominal stop-flow perfusion with gemcitabine in patients with advanced pancreatic cancer and refractory malignant ascites. Cancer Chemother Pharmacol 63: 331-341, 2009.
5. Li XF, Carlin S, Urano M, Russell J, Ling CC and O'Donoghue JA: Visualization of hypoxia in microscopic tumors by immunofluorescent microscopy. Cancer Res 67: 7646-7653, 2007.
6. Driessen A, Landuyt W, Pastorekova S, Moons J, Goethals L, Haustermans K, Nafteux P, Penninckx F, Geboes K, Lerut T, *et al*: Expression of carbonic anhydrase IX (CA IX), a hypoxia-related protein, rather than vascular-endothelial growth factor (VEGF), a pro-angiogenic factor, correlates with an extremely poor prognosis in esophageal and gastric adenocarcinomas. Ann Surg 243: 334-340, 2006.
7. Vander Heiden MG, Cantley LC and Thompson CB: Understanding the Warburg effect: The metabolic requirements of cell proliferation. Science 324: 1029-1033, 2009.
8. Wise DR, Ward PS, Shay JE, Cross JR, Gruber JJ, Sachdeva UM, Platt JM, DeMatteo RG, Simon MC and Thompson CB: Hypoxia promotes isocitrate dehydrogenase-dependent carboxylation of α-ketoglutarate to citrate to support cell growth and viability. Proc Natl Acad Sci USA 108: 19611-19616, 2011.
9. Metallo CM, Gameiro PA, Bell EL, Mattaini KR, Yang J, Hiller K, Jewell CM, Johnson ZR, Irvine DJ, Guarente L, *et al*: Reductive glutamine metabolism by IDH1 mediates lipogenesis under hypoxia. Nature 481: 380-384, 2012.
10. Le A, Lane AN, Hamaker M, Bose S, Gouw A, Barbi J, Tsukamoto T, Rojas CJ, Slusher BS, Zhang H, *et al*: Glucose-independent glutamine metabolism via TCA cycling for proliferation and survival in B cells. Cell Metab 15: 110-121, 2012.
11. Fontaine KA, Sanchez EL, Camarda R and Lagunoff M: Dengue virus induces and requires glycolysis for optimal replication. J Virol 89: 2358-2366, 2015.
12. Munger J, Bajad SU, Coller HA, Shenk T and Rabinowitz JD: Dynamics of the cellular metabolome during human cytomegalovirus infection. PLoS Pathog 2: e132, 2006.
13. Ripoli M, D'Aprile A, Quarato G, Sarasin-Filipowicz M, Gouttenoire J, Scrima R, Cela O, Boffoli D, Heim MH, Moradpour D, *et al*: Hepatitis C virus-linked mitochondrial dysfunction promotes hypoxia-inducible factor 1 alpha-mediated glycolytic adaptation. J Virol 84: 647-660, 2010.
14. Fontaine KA, Camarda R and Lagunoff M: Vaccinia virus requires glutamine but not glucose for efficient replication. J Virol 88: 4366-4374, 2014.
15. Xiao L, Hu ZY, Dong X, Tan Z, Li W, Tang M, Chen L, Yang L, Tao Y, Jiang Y, *et al*: Targeting Epstein-Barr virus oncoprotein LMP1-mediated glycolysis sensitizes nasopharyngeal carcinoma to radiation therapy. Oncogene 33: 4568-4578, 2014.
16. Pillet S, Le Guyader N, Hofer T, NguyenKhac F, Koken M, Aubin JT, Fichelson S, Gassmann M and Morinet F: Hypoxia enhances human B19 erythrovirus gene expression in primary erythroid cells. Virology 327: 1-7, 2004.
17. Vassilaki N, Kalliampakou KI, Kotta-Loizou I, Befani C, Liakos P, Simos G, Mentis AF, Kalliaropoulos A, Doumba PP, Smirlis D, *et al*: Low oxygen tension enhances hepatitis C virus replication. J Virol 87: 2935-2948, 2013.
18. Aghi MK, Liu TC, Rabkin S and Martuza RL: Hypoxia enhances the replication of oncolytic herpes simplex virus. Mol Ther 17: 51-56, 2009.
19. Haque M, Davis DA, Wang V, Widmer I and Yarchoan R: Kaposi's sarcoma-associated herpesvirus (human herpesvirus 8) contains hypoxia response elements: Relevance to lytic induction by hypoxia. J Virol 77: 6761-6768, 2003.
20. Connor JH, Naczki C, Koumenis C and Lyles DS: Replication and cytopathic effect of oncolytic vesicular stomatitis virus in hypoxic tumor cells in vitro and in vivo. J Virol 78: 8960-8970, 2004.

21. Stojdl DF, Lichty BD, tenOever BR, Paterson JM, Power AT, Knowles S, Marius R, Reynard J, Poliquin L, Atkins H, *et al*: VSV strains with defects in their ability to shutdown innate immunity are potent systemic anti-cancer agents. Cancer Cell 4: 263-275, 2003.
22. Nguyên TL, Abdelbary H, Arguello M, Breitbach C, Leveille S, Diallo JS, Yasmeen A, Bismar TA, Kirn D, Falls T, *et al*: Chemical targeting of the innate antiviral response by histone deacetylase inhibitors renders refractory cancers sensitive to viral oncolysis. Proc Natl Acad Sci USA 105: 14981-14986, 2008.
23. Cave DR, Hendrickson FM and Huang AS: Defective interfering virus particles modulate virulence. J Virol 55: 366-373, 1985.
24. Zhou Y, Wen F, Zhang P, Tang R and Li Q: Matrix protein of vesicular stomatitis virus: A potent inhibitor of vascular endothelial growth factor and malignant ascites formation. Cancer Gene Ther 20: 178-185, 2013.
25. Pourgholami MH: YanCai Z, Lu Y, Wang L, and Morris DL: Albendazole: a potent inhibitor of vascular endothelial growth factor and malignant ascites formation in H22 tumor-bearing nude mice. Clin Cancer Res 12: 1928-1935, 2006.
26. Li Q, Wei YQ, Wen YJ, Zhao X, Tian L, Yang L, Mao YQ, Kan B, Wu Y, Ding ZY, *et al*: Induction of apoptosis and tumor regression by vesicular stomatitis virus in the presence of gemcitabine in lung cancer. Int J Cancer 112: 143-149, 2004.
27. Papaconstantinou J and Colowick SP: The role of glycolysis in the growth of tumor cells. I. Effects of oxamic acid on the metabolism of Ehrlich ascites tumor cells in vitro. J Biol Chem 236: 278-284, 1961.
28. Guillaumond F, Leca J, Olivares O, Lavaut MN, Vidal N, Berthezène P, Dusetti NJ, Loncle C, Calvo E, Turrini O, *et al*: Strengthened glycolysis under hypoxia supports tumor symbiosis and hexosamine biosynthesis in pancreatic adenocarcinoma. Proc Natl Acad Sci USA 110: 3919-3924, 2013.
29. Metallo CM, Gameiro PA, Bell EL, Mattaini KR, Yang J, Hiller K, Jewell CM, Johnson ZR, Irvine DJ, Guarente L, *et al*: Reductive glutamine metabolism by IDH1 mediates lipo-genesis under hypoxia. Nature 481:380-384, 2012.
30. Scott DA, Richardson AD, Filipp FV, Knutzen CA, Chiang GG, Ronai ZA, Osterman AL and Smith JW: Comparative metabolic flux profiling of melanoma cell lines: Beyond the Warburg effect. J Biol Chem 286: 42626-42634, 2011.
31. Delgado T, Carroll PA, Punjabi AS, Margineantu D, Hockenbery DM and Lagunoff M: Induction of the Warburg effect by Kaposi's sarcoma herpe svirus is required for the maintenance of latently infected endothelial cel ls. Proc Natl Acad Sci USA 107: 10696-10701, 2010.
32. Vastag L, Koyuncu E, Grady SL, Shenk TE and Rabinowitz JD: Divergent effects of human cytomegalovirus and herpes simplex virus-1 on cellular metabolism. PLoS Pathog 7: e1002124, 2011.
33. Diamond DL, Syder AJ, Jacobs JM, Sorensen CM, Walters KA, Proll SC, McDermott JE, Gritsenko MA, Zhang Q, Zhao R, *et al*: Temporal proteome and lipidome profiles reveal hepatitis C virus-associated reprogramming of hepatocellular metabolism and bioenergetics. PLoS Pathog 6: e1000719, 2010.
34. Ramière C, Rodriguez J, Enache LS, Lotteau V, André P and Diaz O: Activity of hexokinase is increased by its interaction with hepatitis C virus protein NS5A. J Virol 88: 3246-3254, 2014.
35. Loisel-Meyer S, Swainson L, Craveiro M, Oburoglu L, Mongellaz C, Costa C, Martinez M, Cosset FL, Battini JL, Herzenberg LA, *et al*: Glut1-mediated glucose transport regulates HIV infection. Proc Natl Acad Sci USA 109: 2549-2554, 2012.
36. Gonnella R, Santarelli R, Farina A, Granato M, D'Orazi G, Faggioni A and Cirone M: Kaposi sarcoma associated herpesvirus (KSHV) induces AKT hyperphosphorylation, bortezomib-resistance and GLUT-1 plasma membrane exposure in THP-1 monocytic cell line. J Exp Clin Cancer Res 32: 79, 2013.
37. McArdle J, Schafer XL and Munger J: Inhibition of calmodulin-dependent kinase kinase blocks human cytomegalovirus-induced glycolytic activation and severely attenuates production of viral progeny. J Virol 85: 705-714, 2011.
38. Radsak KD and Weder D: Effect of 2-deoxy-D-glucose on cytomegalovirus-induced DNA synthesis in human fibroblasts. J Gen Virol 57: 33-42, 1981.
39. Courtney RJ, Steiner SM and Benyesh-Melnick M: Effects of 2-deoxy-D-glucose on herpes simplex virus replication. Virology 52: 447-455, 1973.
40. Balachandran S, Porosnicu M and Barber GN: Oncolytic activity of vesicular stomatitis virus is effective against tumors exhibiting aberrant p53, Ras, or myc function and involves the induction of apoptosis. J Virol 75: 3474-3479, 2001.
41. Balachandran S, Roberts PC, Kipperman T, Bhalla KN, Compans RW, Archer DR and Barber GN: Alpha/beta interferons potentiate virus-induced apoptosis through activation of the FADD/Caspase-8 death signaling pathway. J Virol 74: 1513-1523, 2000.
42. Liu HL and Chen J: Oncolytic virus as an agent for the treatment of malignant ascites. Cancer Biother Radiopharm 24: 99-102, 2009.
43. Hadaschik BA, Zhang K, So AI, Fazli L, Jia W, Bell JC, Gleave ME and Rennie PS: Oncolytic vesicular stomatitis viruses are potent agents for intravesical treatment of high-risk bladder cancer. Cancer Res 68: 4506-4510, 2008.